Ceramics International 45 (2019) 7916–7922

Contents lists available at ScienceDirect

Ceramics International

journal homepage: www.elsevier.com/locate/ceramint

Surface morphology and microstructure evolution of B_4C ceramic hollow microspheres prepared by wet coating method on a pyrolysis substrate

Ruichong Chen[a,b], Jianqi Qi[a,b], Xiaofeng Guo[d,e], Diyin Ye[a,b], Xiuling Wang[a,b], Qiwu Shi[c], Di Wu[e,f], Zhijun Liao[a,b,*], Tiecheng Lu[a,b,*]

[a] College of Physical Science and Technology, Sichuan University, Chengdu 610064, China
[b] Key Laboratory of Radiation Physics and Technology of Ministry of Education, Sichuan University, Chengdu 610064, China
[c] College of Materials Science and Engineering, Sichuan University, Chengdu 610064, China
[d] Department of Chemistry, Washington State University, Pullman, WA 99164, United States
[e] Alexandra Navrotsky Institute for Experimental Thermodynamics, Washington State University, Pullman, WA 99164, United States
[f] The Gene and Linda Voiland School of Chemical Engineering and Bioengineering, Washington State University, Pullman, WA 99164, United States

ARTICLE INFO

Keywords:
B_4C ceramic hollow microspheres
ICF capsule
Morphology
Microstructure

ABSTRACT

B_4C hollow microspheres have been proposed as one of the promising ignition capsules for inertial confinement fusion (ICF). It is worth noting that the selection of easier-to-remove substrate materials is the key to obtaining B_4C hollow microspheres. In this work, B_4C core-shell microspheres with a uniform structure are prepared by the wet coating method on a PAMS substrate. After the calcination, the complete thermal decomposition of the PAMS substrate leads to a hollow structure B_4C ceramic microsphere. The effects of solid content of coating slurry on the morphology and microstructure of the B_4C core-shell microspheres were investigated in detail. The result shows that the spacing of the B_4C particles in the slurry gradually decreases with increasing the solid content, resulting in an increase in the surface tension of the slurry and an improved stabilization, which helps to optimize the surface roughness and sphericity of the B_4C microspheres.

1. Introduction

Inertial confinement fusion (ICF) has been proposed as a promising option to realize controlled thermonuclear fusion [1–3]. As one of the key components of ICF, the preparation technology of ignition capsule attracted substantial attention [4–6]. According to the design requirements of the National Ignition Facility (NIF), the ignition capsule should be primarily made by low Z materials such as CH with Br dopant, Be with Cu dopant, glow discharge polymer (GDP), Al_2O_3 or boron carbide (B_4C) [7–11]. Particularly among these materials, B_4C does not need doping but has high hardness, excellent thermal stability and enough opacity under 300 eV, which makes B_4C a promising potential ablator material [12–16]. Moreover, the NIF project has many strict design requirements for the wall thickness, sphericity and surface roughness of B_4C ignition capsules [17]. Unfortunately, to the best of author's knowledge, there are few reports describing the fabrication of B_4C ignition capsule that meets NIF design requirement.

In previous work [18], we presented a rapid method to prepare a B_4C ceramic double-curvature shell with a high uniformity by dropping the coating slurry on molybdenum (Mo) substrate. Subsequently, the double-curvature shell needs to be soaked in aqua regia to remove the Mo substrate to obtain the B_4C microspheres with a hollow structure. However, in the following studies, we found that the reaction between aqua regia and Mo was too aggressive, with a large number of bubbles generating during the reaction that can easily damage the B_4C shells, resulting in low yield of B_4C hollow microspheres. Therefore, the selection of easier-to-remove substrate materials is an urgent problem that we need to solve. Remarkably, Tang et al. reported the preparation of SiC hollow microspheres on a poly(α-methylstyrene) (PAMS) substrate by the chemical vapor deposition (CVD) [19]. It should be noted that the PAMS substrate can be completely removed at 300 °C [20], which provides a new substrate choice for the preparation of B_4C ceramic hollow microspheres.

In this work, we present a novel approach to fabricate B_4C ceramic hollow microspheres. First, the B_4C slurry was prepared by Isobam gelling system. Then the as-prepared slurry was poured on a PAMS substrate to form a core-shell structure B_4C microspheres. Finally, the core-shell structured B_4C microsphere was processed by pyrolysis and

* Corresponding authors at: College of Physical Science and Technology, Sichuan University, Chengdu 610064, China.
E-mail addresses: liaozhijun@scu.edu.cn (Z. Liao), lutiecheng@scu.edu.cn (T. Lu).

https://doi.org/10.1016/j.ceramint.2019.01.103
Received 11 October 2018; Received in revised form 9 January 2019; Accepted 14 January 2019
Available online 15 January 2019

densification to obtain the B_4C ceramic hollow microsphere, followed by the detail characterizations of the morphology, microstructure, composition, surface roughness and sphericity.

2. Experimental

2.1. Starting materials

During the sample preparation, a commercial B_4C powder (1–3 μm, Aladdin, Shanghai, China) was used as the raw material. The Isobam-104 (Kuraray, Osaka, Japan) was used as both the gelling agent and dispersant. PAMS spheres with a diameter of 1 mm prepared by the droplet generator technique were used as the substrate [20].

2.2. Synthesis of the B_4C ceramic hollow microsphere

The schematic diagram to fabricate B_4C ceramic hollow microspheres is shown in Fig. 1. First, B_4C powder and Isobam-104 were added into deionized water followed by a ball-milling with agate balls for 2 h at a rotate speed of 250 r/min to obtain the B_4C slurry containing 32.4–41.9 vol% solid content. The mass ratio of B_4C powder, deionized water and Isobam-104 was 240/280/320/360:200:1. Second, the B_4C slurry was extruded from a syringe and dropped on a PAMS substrate, which is fixed on a capillary with a diameter of 0.1 mm. Due to the influence of gravity, the slurry will converge toward the bottom of the substrate, causing the coating in the bottom to be thicker than those in other positions. It should be noted that the capillary can drain the excess slurry at the bottom of the substrate, helping to reduce the effects of gravity. The B_4C slurry eventually formed a nearly uniform spherical coating on the PAMS substrate. In addition, the hole formed by the capillary on the microsphere can also provide a channel for subsequent D-T fuel filling. Last, the core-shell B_4C microspheres were heated to 500 °C for 4 h to remove the PAMS substrate and Isobam-104 in flowing oxygen, and then calcined at 1600 °C for 5 h under N_2 to obtain the B_4C ceramic hollow microspheres.

2.3. Characterization

The morphologies, microstructures and wall thickness were characterized by scanning electron microscopy (SEM, Model S-4800, Hitachi, Japan). The surface roughness was analyzed by an atomic force microscope (AFM, DI-EnviroScope, Veeco Instruments). X-ray diffraction (XRD, DX-2700) was employed to investigate the phase constituent. The sphericity and uniformity were measured through calculation [21]. We obtained 10 diameter values of the microspheres by random measurement. Extract the maximum (L_{max}) and minimum values (L_{min}), and calculate the average value (L_{ave}). Finally, the sphericity (s) was calculated by the following formula:

$$s = \left(1 - \frac{L_{max} - L_{min}}{L_{ave}}\right) \times 100\% \quad (1)$$

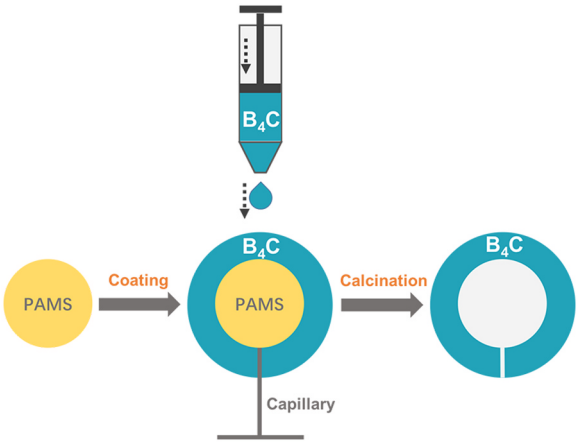

Fig. 1. Schematic diagrams of the experimental setup.

3. Results and discussion

3.1. SEM study of the B_4C core-shell microspheres

Fig. 2 shows the SEM morphology and microstructure of the B_4C core-shell microspheres prepared by the B_4C slurry with different solid contents (32.4 vol%, 35.9 vol%, 39.0 vol% and 41.9 vol%). It can be seen from Fig. 2(a-c) that there were many convex holes and micro-cracks on the surface of the B_4C core-shell microspheres prepared by the slurry with 32.4 vol%, and the length of the hole was ~12 μm. The reason for this phenomenon is mainly due to the hydrophobic nature of the PAMS surface, therefore, it is difficult for the slurry with a low solid content to form a continuous coating on its surface. Fig. 2(d-f) are the SEM images of the B_4C core-shell microspheres prepared by the slurry with 35.9 vol%, there were still many convex holes and micro-cracks on the surface of the microsphere, though with the hole size being reduced to ~6 μm. As the solid content of the slurry increasing to 39.0 vol% (Fig. 2(g-i)), the convex holes on the microsphere surface have completely disappeared, with obtaining a continuous spherical coating. These results indicate that increasing the solid content may gradually offset the influence of the hydrophobic substrate. Fig. 2(j-l) show the B_4C core-shell microsphere prepared by the slurry with 41.9 vol%. In order to directly examine the combination of the B_4C coating and the substrate, we destroyed some of the coatings by external forces (Fig. 2(k)). It can be observed that a quite smooth and uniform B_4C coating was wrapped on the PAMS substrate. In addition, from Fig. 2(l), it can be seen that all B_4C particles were more compact and no large defects has been found in the coating.

3.2. AFM study of the B_4C core-shell microspheres

In order to study the morphology evolution of B_4C microspheres from the atomic scale, we used AFM to analyze the sample morphology. Fig. 3 shows the 3D AFM micrographs of the B_4C core-shell microspheres prepared by the B_4C slurry with different solid contents ranging from 32.4 to 41.9 vol%. We check the surface roughness by averaging the AFM results from two separated areas around the microsphere. The surface root mean square roughness (RMS) is defined as the standard deviation of the surface height profile from the average height [22], measured within the fixed area of 5 μm × 5 μm. As shown in the figure, the variation of the solid content of the slurry affects the surface of B_4C core-shell microspheres. Fig. 3(a) and (b) present the AFM images of the B_4C core-shell microspheres prepared by the slurry with 32.4 vol%, which exhibits quite rough surfaces with many irregular sharp bulges and an average RMS of 339.0 nm. As the solids content of the slurry increasing to 35.9 vol%, the sharp bulges on the surface of the microspheres are converted to more gentle bulges, with a decreased average RMS of 285.3 nm. Continuing increasing the solid content of the slurry from 35.9 to 39.0 vol% leads to the almost removal of the bulges on the surface of the microspheres which is replaced by horizontal folds (157.1 nm average RMS). Also, we find that the B_4C core-shell microspheres with an average RMS of 103.0 nm can be obtained by the slurry with 41.9 vol%, as shown in Fig. 3(g) and (h). All results indicate that there is a positive correlation between the solids content of the slurry and the smoothness and/or the flatness of the spherical coating on the PAMS substrate.

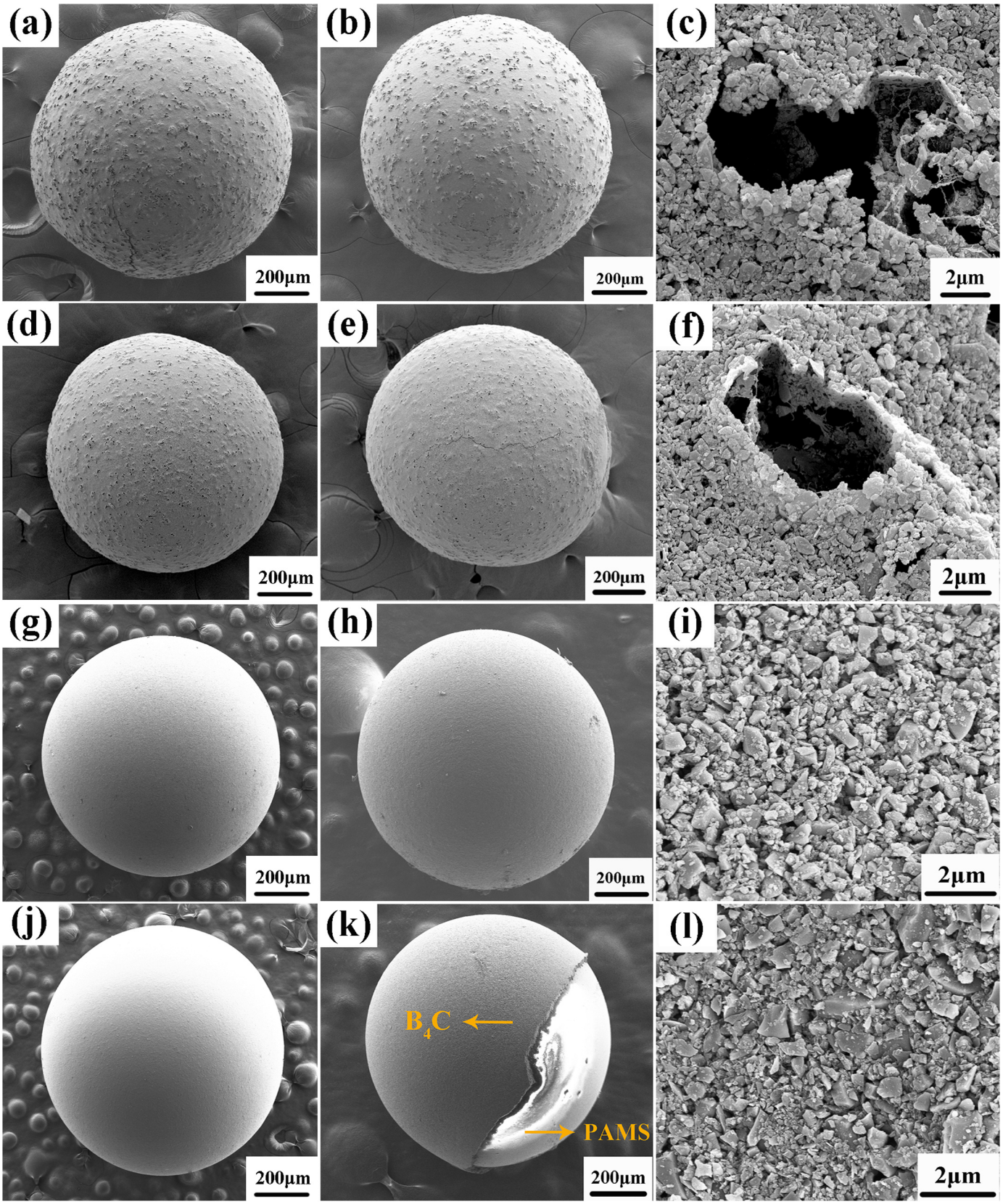

Fig. 2. SEM morphology and microstructure of the B_4C core-shell microspheres prepared by the B_4C slurry with different solid content: (a-c) 32.4 vol%; (d-f) 35.9 vol %; (g-i) 39.0 vol%; (j-l) 41.9 vol%.

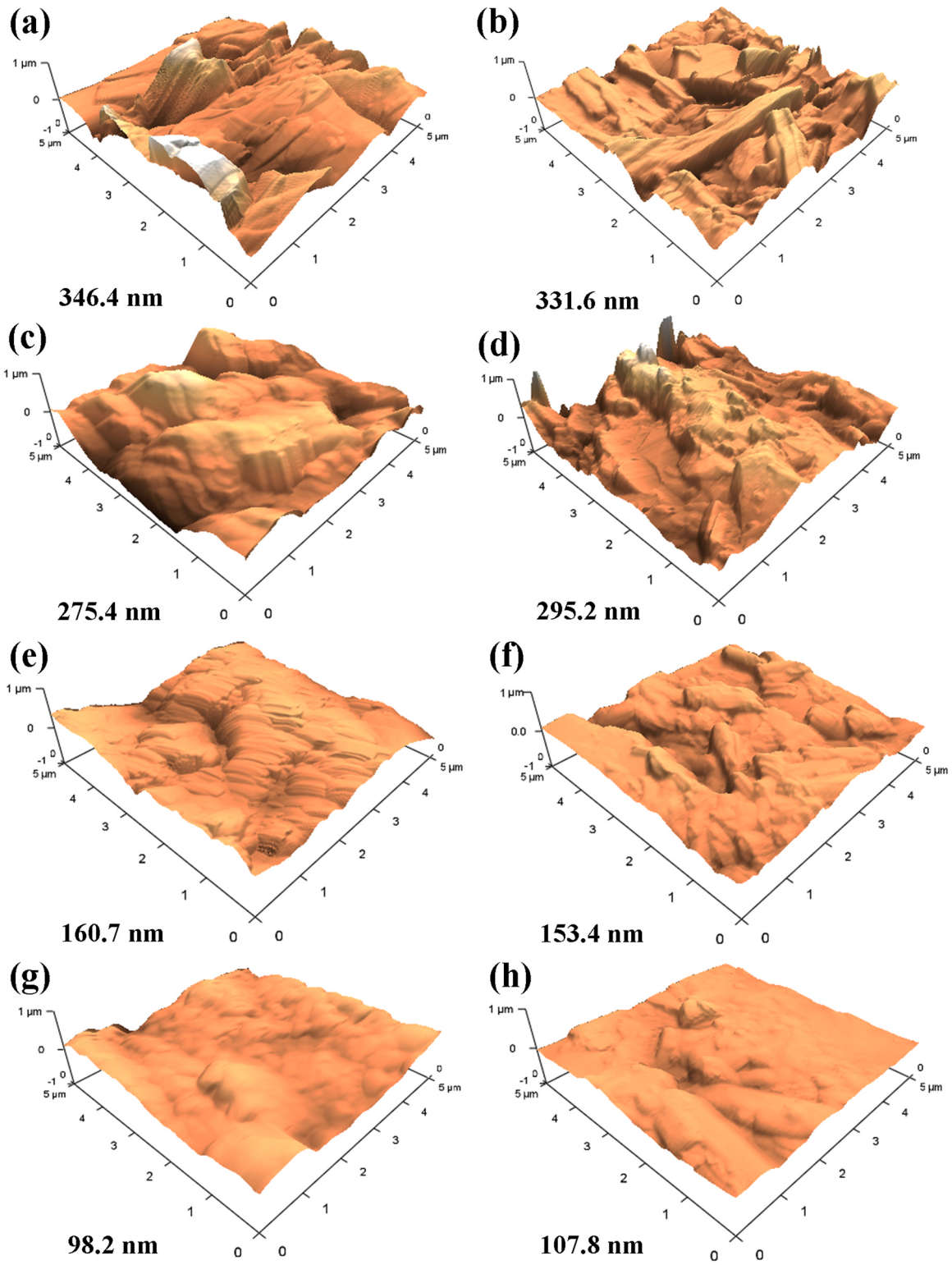

Fig. 3. 3D AFM micrographs of the B_4C core-shell microspheres prepared by the B_4C slurry with different solid content: (a-b) 32.4 vol%; (c-d) 35.9 vol%; (e-f) 39.0 vol %; (g-h) 41.9 vol%.

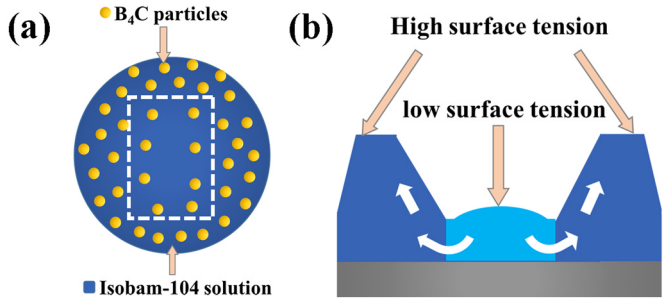

Fig. 4. (a-b) Schematic diagram of forming a coating from B_4C slurry with low solid content.

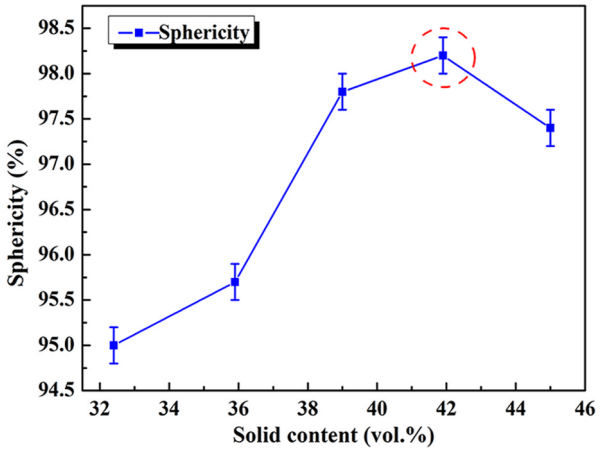

Fig. 5. The effect of solid content on the sphericity of the B_4C core-shell microspheres.

3.3. Physical description of the coating process

In the slurry of the water system, the content of solid particles will directly affect the surface tension of the slurry [23]. To better explain this phenomenon, we developed a physical description of the coating process. As shown in Fig. 4(a), the B_4C particles are relatively loosely dispersed in the slurry with a low solid content, and the large space between the particles causes a heterogeneous surface tension of slurry that leads to the formation of both the low surface tension region (white dotted area) and the high surface tension region. During the coating process, the slurry in the low surface tension region tended to migrate to the surrounding high surface tension region, forming a convex hole (Fig. 4(b)). Noted that with increasing the solid content of the slurry, the spacing of the B_4C particles in the slurry gradually decreases, resulting in an increase in surface tension of the slurry and a gradual stabilization, which helps to obtain a flatter coating.

3.4. Effect of solid content on the sphericity of the B_4C core-shell microspheres

Fig. 5 shows the effect of solid content on the sphericity of the B_4C core-shell microspheres. It can be observed from the diagram that the sphericity of the microsphere improves with the increase of the solid content of the slurry in the range of 32.4–41.9 vol%. It is remarkable that the sphericity of the B_4C core-shell microspheres prepared by the slurry with 41.9 vol% is 98.2 ± 0.2%. However, further increasing the solid content of the slurry leads to a decrease in the sphericity of the microspheres, which could be due to the difficulty of keeping the slurry with a high solid content at a stable viscosity during the coating process. Thus, we conclude that 41.9 vol% is the optimum solid content of the slurry to form the B_4C core-shell microspheres with minimizing surface roughness and maximizing sphericity.

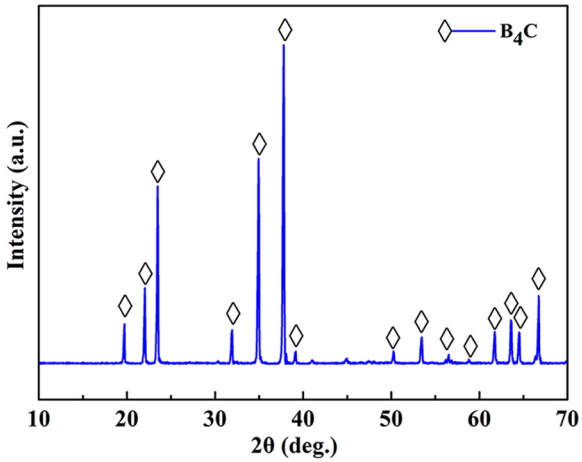

Fig. 6. The XRD pattern of the B_4C microspheres prepared by the slurry with 41.9 vol% and calcined at 1600 °C.

3.5. Hollowing of the B_4C core-shell microspheres

In order to realize the hollowing of core-shell microspheres and improve their mechanical properties, the B_4C core-shell microspheres prepared by the slurry with 41.9 vol% were firstly heated to 500 °C in air to eliminate the organics and then calcined at 1600 °C under the N_2 to achieve the densification. The calcination temperature beyond 1600 °C is not considered because of the decrease in the sphericity of the microspheres. The XRD pattern of the B_4C microspheres prepared by the slurry with 41.9 vol% and calcined at 1600 °C is shown in Fig. 6. It can be seen from the figure that the organics in the microspheres have been completely removed. Moreover, most of the diffraction peaks in the pattern can be indexed by JCPDS card No. 35-0798, indicating that a high purity of the as-prepared B_4C ceramic hollow microspheres.

Fig. 7(a-c) are the SEM images of B_4C ceramic hollow microspheres prepared by the slurry with 41.9 vol% and calcined at 1600 °C. The holes on the surface of the microspheres are obtained through the physical destruction, so as to better observe the hollow structure. It can be seen from the figure that the surface of the microspheres becomes relatively rough during the high-temperature densification. Moreover, the size of B_4C particles did not grow significantly during the densification, and the shape of particles tended to be spheroidal. Fig. 7(d) shows the cross-section of the B_4C ceramic hollow microsphere, with a wall thickness of ~120 μm. Table 1 lists the diameter and wall thickness of the B_4C hollow microspheres calcined at 1600 °C. By calculating the data in Table 1, the sphericity and uniformity of the hollow microspheres were measured to be 97.9% and 95.9%, respectively [21]. In addition, Fig. 8 shows the 3D AFM micrographs from two separated areas around the B_4C hollow microspheres. The average RMS of B_4C hollow microspheres calcined at 1600 °C increases only from 103.0 nm to 193.1 nm. All results indicate that B_4C ceramic hollow microspheres with uniform structure and high sphericity can be obtained by this wet coating method on PAMS substrate.

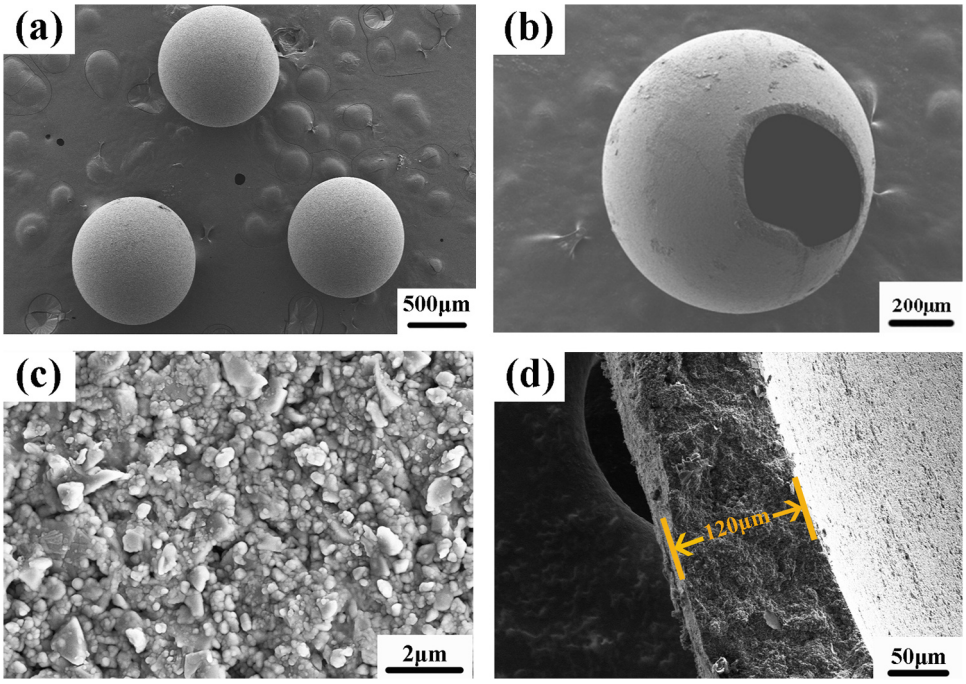

Fig. 7. (a-c) The SEM morphology of the surface and (d) cross-section of the B_4C microspheres prepared by the slurry with 41.9 vol% and calcined at 1600 °C.

Table 1
Diameter and wall thickness of the B_4C microspheres prepared by the slurry with 41.9 vol% and calcined at 1600 °C.

No.	Diameter (μm)	Wall thickness (μm)
1	1150.4	123.1
2	1140.6	118.2
3	1145.7	119.8
4	1164.2	120.5
5	1155.1	122.6
Mean	1151.2	120.8

4. Conclusion

In this work, we described a successful approach preparing the B_4C ceramic hollow microsphere by the wet coating method on a PAMS substrate. The PAMS core was removed completely through the heat treatment. The surface morphology and microstructure can be effectively optimized by adjusting the solid content of the coating slurry. The result shows that the B_4C slurry with a low solid content causes the uneven surface tension, forming heterogeneous regions of various tensions. During the coating process, the slurry in the low surface tension region migrates to the surrounding high surface tension region, forming a convex hole. Remarkably, we found that increasing the solid content of the slurry helps obtain the B_4C coating with an improved flatness. The RMS roughness of the B_4C core-shell microspheres can be decreased from 346.3 to 98.2 nm by increasing the solid content of the slurry from 32.4 to 41.9 vol%. Moreover, B_4C core-shell microspheres with sphericity of 98.2 ± 0.2% can be obtained at the 41.9 vol% solids content. The B_4C hollow ceramic microspheres with a wall thickness of ~120 μm can be obtained through the thermal decomposition and densification. Furthermore, our fabrication technique can facilitate future studies of fabricating ceramic microspheres with hollow microstructures.

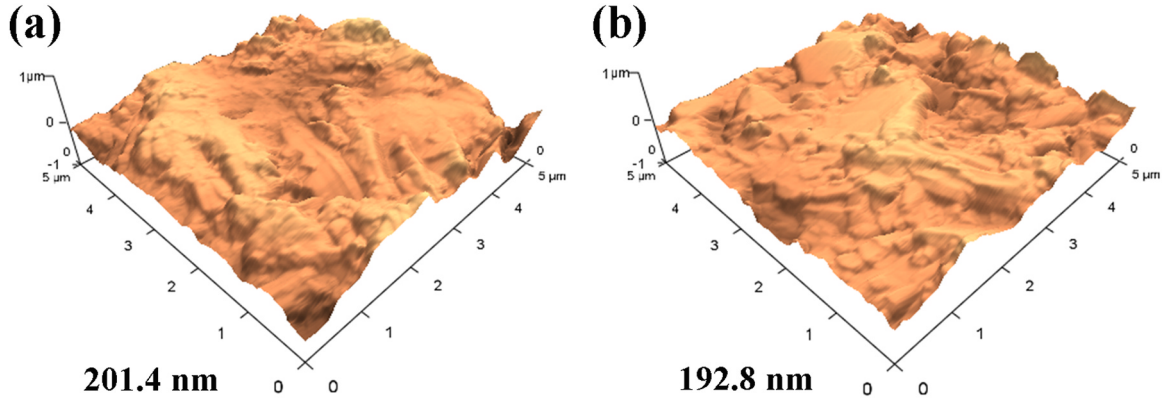

Fig. 8. 3D AFM micrographs of the B_4C microspheres prepared by the slurry with 41.9 vol% and calcined at 1600 °C.

Acknowledgments

This work was supported by the ITER Program (No. 2014GB125002), the Major Science and Technology Programs of China, the National Natural Science Foundation of China under Grant nos. 11505122 and 11775152, and the National High Technology Research and Development Program (863). The authors would like to thank Lingzhu Yu (National Engineering Research Center for Biomaterials, Sichuan University) for help in characterizing SEM.

References

[1] D. Keefe, Inertial confinement fusion, Annu. Rev. Nucl. Part. Sci. 32 (1) (1982) 391–441.
[2] J. Lindl, Development of the indirect-drive approach to inertial confinement fusion and the target physics basis for ignition and gain, Phys. Plasmas 2 (11) (1995) 3933–4024.
[3] J.J. Duderstadt, G.A. Moses, Inertial Confinement Fusion, John Wiley & Sons, 1982.
[4] Y. Zeng, F. Wang, Q. Liao, H. Liu, X. Li, Synthesis and characterization of translucent MgO-doped Al2O3 hollow spheres in millimeter-scale, J. Alloy. Compd. 608 (2014) 185–190.
[5] K.A. Moreno, S. Eddinger, J. Fong, Y.T. Lee, A. Nguyen, A. Nikroo, H. Huang, R. Rosano, H.W. Xu, Overview of national ignition facility capsule metrology, Fusion Sci. Technol. 55 (4) (2009) 349–355.
[6] S.W. Haan, D.A. Callahan, M.J. Edwards, B.A. Hammel, D.D. Ho, O.S. Jones, J.D. Lindl, B.J. MacGOWAN, M.M. Marinak, D.H. Munro, S.M. Pollaine, J.D. Salmonson, B.K. Spears, L.J. Suter, Rev3 update of requirements for NIF ignition targets, Fusion Sci. Technol. 55 (3) (2009) 227–232.
[7] L. Zhang, X. He, G. Chen, T. Wang, Y. Tang, Z. He, Effects of rf power on chemical composition and surface roughness of glow discharge polymer films, Appl. Surf. Sci. 366 (2016) 499–505.
[8] H. Wang, F. Wang, Q. Liao, X. Li, Synthesis of millimeter-scale Al2O3 ceramic hollow spheres by an improved emulsion microencapsulation method, Ceram. Int. 41 (3) (2015) 4959–4965.
[9] Alan K. Burnham, Michael T. Tobin, Andrew T. Anderson, Eric C. Honea, Kenneth M. Skulina, David Milam, Mark Evans, Frank Rainer, Michel Gerassimenko, Development and evaluation of first wall materials for the national ignition facility, Fusion Technol. 30 (3P2A) (1996) 730–735.
[10] A. Nikroo, F.H. Elsner, D.G. Czechowicz, J. Gibson, S.E. Grant, A.L. Greenwood, M.L. Hoppe, D. Husband, B.W. Mcquillan, W.J. Miller, J.M. Pontelandolfo, D.A. Steinman, R.B. Stephens, K.R. Schultz, M. Takagi, Capsule Production And Development for ICF Experiments. General Atomics Report GA-A23228, (1999).
[11] R. Chen, Q. Shi, L. Su, M. Yang, Z. Huang, Y. Shi, Q. Zhang, Z. Liao, T. Lu, Preparation of a B4C hollow microsphere through gel-casting for an inertial confinement fusion (ICF) target, Ceram. Int. 43 (1) (2017) 571–577.
[12] P.A. Medwick, H.E. Fischer, R.O. Pohl, Thermal conductivity and specific heat of boron carbides[J], J. Alloy. Compd. 203 (1–2) (1994) 67–75.
[13] R. Chen, L. Su, J. Qi, Q. Shi, Y. Shi, Z. Liao, T. Lu, Effect of deposition time on the growth mode and stoichiometric of amorphous boron carbide thin films deposited by electron beam evaporation, Ceram. Int. (2018).
[14] A. Alizadeh, E. Taheri-Nassaj, N. Ehsani, Synthesis of boron carbide powder by a carbothermic reduction method, J. Eur. Ceram. Soc. 24 (10–11) (2004) 3227–3234.
[15] F. Thevenot, Boron carbide—a comprehensive review, J. Eur. Ceram. Soc. 6 (4) (1990) 205–225.
[16] T.R. Dittrich, S.W. Haan, S. Pollaine, A.K. Burnham, G.L. Strobel, NIF capsule design update, Fusion Technol. 31 (4) (1997) 402–405.
[17] Alan K. Burnham, Craig S. Alford, Daniel M. Makowiecki, Thomas R. Dittrich, Russell J. Wallace, Eric C. Honea, Charlotte M. King, David Steinman, Evaluation of B4C as an Ablator material for NIF capsules, Fusion Technol. 31 (4) (1997) 456–462.
[18] R. Chen, J. Qi, L. Su, Q. Shi, X. Guo, D. Wu, T. Lu, Z. Liao, Rapid preparation and uniformity control of B4C ceramic double-curvature shells: aim to advance its applications as ICF capsules, J. Alloy. Compd. 762 (2018) 67–72.
[19] C. Tang, Z. He, X. He, J. Huang, Y. Yi, H. Wang, T. Wang, Preparation and characterization of SiC hollow microspheres, Mater. Lett. 207 (2017) 104–108.
[20] B.W. McQuillan, A. Nikroo, D.A. Steinman, F.H. Elsner, D.G. Czechowicz, M.L. Hoppe, M. Sixtus, W.J. Miller, The PAMS/GDP process for production of ICF target mandrels, Fusion Technol. 31 (4) (1997) 381–384.
[21] M. Liu, S. Chen, Y. Liu, L. Su, R. Shi, X. Qi, B. Li, Z. Zhang, Characterization of sphericity and wall thickness uniformity of thick-walled hollow microspheres, High. Power Laser Part Beams 26 (2014) 153–157.
[22] E.S. Gadelmawla, M.M. Koura, T.M.A. Maksoud, I.M. Elewa, H.H. Soliman, Roughness parameters, J. Mater. Process. Technol. 123 (1) (2002) 133–145.
[23] B.W. Brian, J.C. Chen, Surface tension of solid-liquid slurries, AIChE J. 33 (2) (1987) 316–318.